PAWLEY, G. S., MACKENZIE, G. A., BOKHENKOV, E. L., SHEKA, E. F., DORNER, B., KALUS, J., SCHMELZER, U. & NATKANIEC, I. (1980). *Mol. Phys.* **39**, 251–260.
PAWLEY, G. S. & WILLIS, B. T. M. (1970). *Acta Cryst.* A**26**, 260–262.
PAWLEY, G. S. & YEATS, E. A. (1969). *Acta Cryst.* B**25**, 2009–2013.
PRINCE, E. & FINGER, L. W. (1973). *Acta Cryst.* B**29**, 179–183.
SCHERINGER, C. (1972*a*). *Acta Cryst.* A**28**, 512–515.
SCHERINGER, C. (1972*b*). *Acta Cryst.* A**28**, 516–521.
SCHERINGER, C. (1972*c*). *Acta Cryst.* A**28**, 616–619.
SCHERINGER, C. & FADINI, A. (1979). *Acta Cryst.* A**35**, 610–613.
SCHETTINO, V. (1967). *J. Chem. Phys.* **46**, 302–309.
SCHETTINO, V., NETO, N. & CALIFANO, S. (1966). *J. Chem. Phys.* **44**, 2724–2734.
SCHOMAKER, V. & TRUEBLOOD, K. N. (1968). *Acta Cryst.* B**24**, 63–76.
SCULLY, D. B. & WHIFFEN, D. H. (1960). *Spectrochim. Acta*, **16**, 1409–1415.
STØLEVIK, S., SEIP, H. M. & CYVIN, S. J. (1972). *Chem. Phys. Lett.* **15**, 263–265.
SUZUKI, M., YOKOYAMA, T. & ITO, M. (1968). *Spectrochim. Acta Part A*, **24**, 1091–1107.
TADDEI, G., BONADEO, H., MARZOCCHI, M. P. & CALIFANO, S. (1973). *J. Chem. Phys.* **58**, 966–978.
WHITMER, J. C., CYVIN, S. J. & CYVIN, B. N. (1978). *Z. Naturforsch. Teil A*, **33**, 45–54.
WILLIAMS, D. E. (1967). *J. Chem. Phys.* **47**, 4680–4684.
WILLIS, B. T. M. & HOWARD, J. A. K. (1975). *Acta Cryst.* A**31**, 514–520.
WILLIS, B. T. M. & PAWLEY, G. S. (1970). *Acta Cryst.* A**26**, 254–259.
WILLIS, B. T. M. & PRYOR, A. W. (1975). *Thermal Vibration Analysis in Crystallography*. Cambridge Univ. Press.

Acta Cryst. (1982). A**38**, 356–362

The Observation of Molecular Orientations in Crystal Defects and the Growth Mechanism of Thin Phthalocyanine Films

BY TAKASHI KOBAYASHI, YOSHINORI FUJIYOSHI AND NATSU UYEDA

Institute for Chemical Research, Kyoto University, Uji, Kyoto-Fu 611, *Japan*

(*Received* 23 *October* 1981; *accepted* 18 *January* 1982)

Abstract

The crystal imperfections in very thin films of metal-phthalocyanines were observed by means of high-resolution electron microscopy. It was revealed that the anisotropic molecular shape played an important role in the formation of the defect and grain boundaries. The quasi-amorphous state of phthalocyanine was found in which the existence of a linear crystal, a molecular column, was confirmed in the early stages of the formation of the three-dimensional crystal.

Introduction

The energy structure as well as the electrical and photo-conductive properties of molecular crystals cannot fully be interpreted without considering the local structures of the crystal, because the local lattice irregularities have the possibility to act as traps for electrons. Therefore, information about the local structure having certain irregularities, such as point, line, planar and bulk defects, is required for organic crystals by those who intend to develop organic materials for practical use. The properties of such defects in molecular crystals fundamentally differ from those in covalent or metallic crystals because of the anisotropy of intermolecular forces and of the shapes of the molecules. The differences also cause various peculiarities in growth mechanisms of the crystal. Investigations of defects in organic crystals have been carried out by Williams, Thomas, Williams & Hobbs (1975) on the basis of diffraction contrast in electron micrographs and by Fryer (1977) by the use of molecular imaging. In the present investigation, not only the defect structures but also the growth mechanisms of phthalocyanine crystals have been revealed through a direct observation of molecular images by means of high-resolution electron microscopy with the aid of an automatic minimum-dose system, which has been developed by the present authors (Fujiyoshi, Kobayashi, Ishizuka, Uyeda, Ishida & Harada, 1980) in order to avoid the deterioration of the images due to the radiation damage of the crystal. In the section discussing the growth mechanism, a quasi-amorphous or precrystalline state will be shown as the early stage of the crystal growth.

0567-7394/82/030356-07$01.00

Experimental

Purified samples of zinc-, copper- and platinum-phthalocyanines (Zn-Phc, Cu-Phc, Pt-Phc) were sublimed from a quartz crucible heated at about 500 °C in a vacuum of 4×10^{-5} Pa and deposited at room temperature onto very thin carbon films fixed on gold-coated microgrids. The specimen thickness was monitored by a quartz crystal microbalance so as to have a mean value of 10, 25 or 50 Å. The thickness of the substrate carbon film, prepared by the indirect deposition technique, was determined by electron microscopy to be 30 Å. The observation was performed by the use of a JEM-100C electron microscope equipped with a high-resolution objective pole piece ($C_s = 0{\cdot}7$ mm) and operated at 100 kV and a JEM-200 ($C_s = 1{\cdot}2$ mm) operated at 200 kV. The direct working magnifications were 170 000 and 100 000.

Results and discussion

(1) *Planar defects*

Planar defects in the Phc crystals were observed in the form of stacking faults or grain boundaries. One example of a stacking fault found in a crystal of Cu-Phc is shown in Fig. 1, which is a projection on the plane including the crystal *b* axis. In this projection the molecules are viewed along the molecular planes and imaged as dark stakes. These stakes stack to form columns along one direction, defined as the crystal *b* axis, and are inclined at $\pm 60°$ to the axis. The direction of the inclination usually alternates from column to column.

However, one column of the molecular images is apparently misaligned as indicated by a box in Fig. 1. The misaligned column produces a half-period shift along the *b* axis and is considered to be a stacking fault in terms of the molecular column. Phthalocyanine molecules are apt to pile up in a direction almost perpendicular to the molecular plane because the anisotropic intermolecular force acts more strongly in this direction through the π electronic interactions between two adjacent molecules. The packing drawing of the molecules and two projections of the column are shown in Fig. 2. The angle between the column axis and the molecular plane is constant in a particular crystal modification and differs between polymorphs. The angles obtained for the α-Pt-Phc and the β-Cu-Phc are 25·3° and 45·8° respectively, as reported by Brown (1968). The angle obtained for the present specimen is 30°, like that in α-Pt-Phc. The α-Pt-Phc analysed by X-ray diffraction by Brown (1968) belongs to the space group $C2/c$, which requires that the projection onto a plane including the *b* axis should

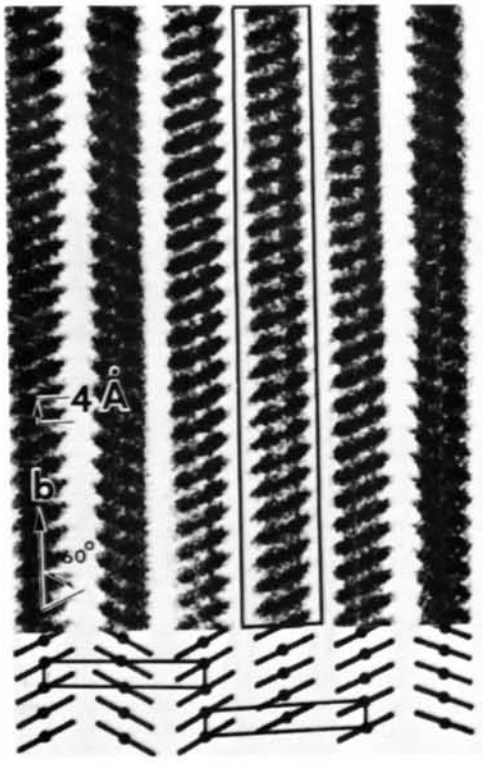

Fig. 1. The structure image of Zn-Phc in the projection *B*. The molecular layer enclosed is misoriented and shifted by a half period along the *b* axis.

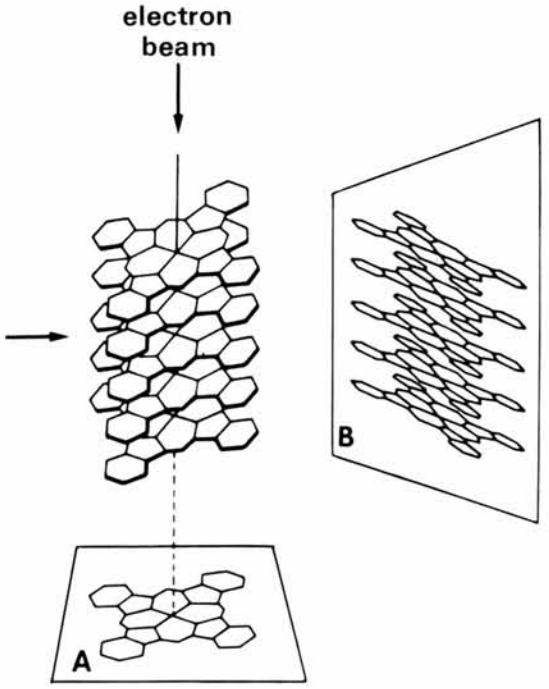

Fig. 2. Illustration of a molecular column of Phc and its two projections. In the projection *A* along the column, the column is seen as a molecule in Greek chi (χ) shape and in the side projection *B* the molecules look like stakes when the resolution of electron microscope used is about 3·0 Å.

make the molecular interval one half of the unit-cell constant along the b axis. The image shown in Fig. 1 exhibits the intermolecular distance of 4 Å and indicates that this crystal belongs to another space group, being a polymorph different from the α form. The existence of new polymorphs in the vacuum-deposited film has been reported by Kobayashi, Fujiyoshi, Iwatsu & Uyeda (1981). The stacking irregularity of the molecular columns can be frequently observed in high-resolution electron micrographs of phthalocyanine thin films. This fact suggests that this stacking disorder can easily happen in the crystals and the change in the lattice energy due to the disorder may not be too large. It is also assumed that the change in the lattice energy can be reduced by a displacement of misaligned molecular columns along the axis, as is observed in Fig. 1.

Another planar defect was observed as a grain boundary. The image shown in Fig. 3 exhibits a grain boundary. The image contrasts and the crystal shape are of great interest from the view point of crystal growth and will be discussed in § 4. It can be observed in Fig. 3 that the molecular orientation in the upper side of the boundary XX' is reversed relative to that in the lower part. The molecules on the line XX' take a different orientation from the molecules both in the upper and lower parts. The lattice displacement along the boundary can also be seen in the image. This displacement and the inversion of molecular orientation are considered to be in cross correlation. If the slip only occurs in the plane exhibiting the molecular image, as in Fig. 3, and the displacement distance is a half period along the slip plane, the boundary becomes very unstable owing to the steric hindrance on the slip plane, as shown in Fig. 4(*a*). Such a boundary cannot possibly exist. However, when the slip is accompanied by a rotational displacement around each molecular center, in the lower half of the crystal such steric hindrance can be avoided, as shown in Fig. 4(*c*), which is the same situation as with the real images shown in Fig. 3. If two crystals with inverse molecular orientations make a boundary without any lattice displacement along this boundary, a similar unstable configuration may be formed at the boundary (Fig. 4*b*). In this case the displacement of a half period along the boundary is necessary to diminish the repulsive forces between two adjacent molecules in each side of the boundary. Thus the parallel displacement of half the crystal, *i.e.* slip, and the rotational displacement of molecules should

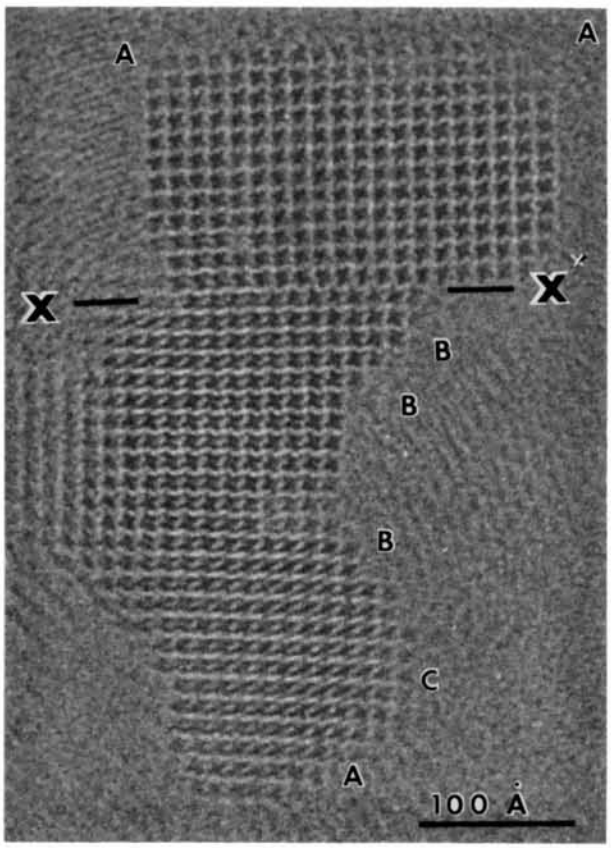

Fig. 3. The grain boundary XX' is shown. The molecular images at the crystal corners A and the kink B differ in contrast from those at the crystal midpoint. The molecules at the corners are, in general, weakly bound to the crystal and can easily be released. In an equilibrium state, kink B should be filled by molecules. The crystal edge C also shows faint and diffuse images. Contrast differences in the molecular images correspond to the differences in numbers of molecules contributing to the formation of each image.

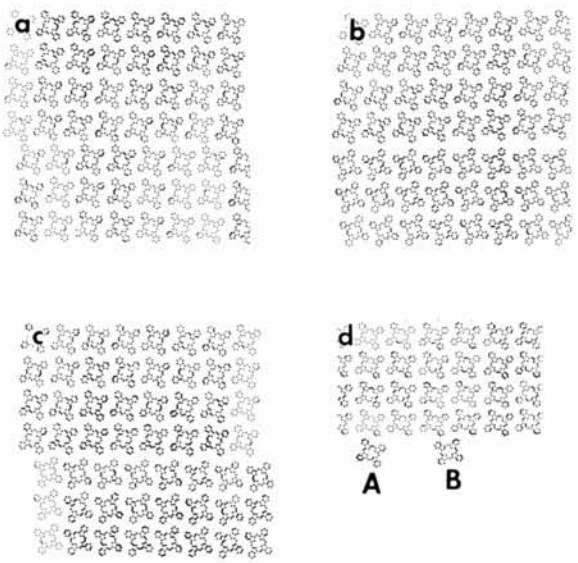

Fig. 4. A schematic explanation of the grain boundary shown in Fig. 2. The slipped state (*a*) and the rotational displacement of molecules in the half crystal (*b*) cannot exist because of the steric hindrance of the adjacent phenyl groups. A combination of the parallel and rotational displacements makes the boundary stable, as shown in (*c*). Two possible sites for molecules at the growth front (*d*) are also shown.

occur together in order to make the grain boundary stable, as shown in Fig. 3. However, the grain boundary displayed in Fig. 3 was not generated by any stress applied on the crystal, but formed during the growth process. Therefore the following mechanism is plausible for the formation of such a grain boundary. When the plane XX' is considered to have been a growth front of the crystal, there are two possible sites on the front for a molecule coming to join the crystal, as illustrated in Fig. 4(*d*). One is the site *A* from which the normal regular lattice will be formed and the other is the site *B* at which the molecule added takes a different orientation from that in the mother crystal. The orientation is reversed at the site *B* and the boundary shown in Fig. 3 will be produced. The mechanism of grain-boundary formation described here can also be useful for considering twin formation and will be discussed again later. Fig. 5 is an example which can be considered as a bulk defect. The defect is composed of a small crystalline inclusion around which a grain boundary of the type discussed above is observed. An inclusion like this can also be generated by the same mechanism. It is inferred that the rapid growth rate of the mother crystal suppresses the growth of the crystalline part with an inverse molecular orientation and surrounds the disordered part, which forms an inclusion.

(2) *Line defects and point defects*

Line defects in crystals are dislocations. Edge dislocations are the most common defects in organic crystals. A structure image containing an edge dislocation is shown in Fig. 6, which is a projection of the crystal along the molecular column axis, that is the molecular columns stand normal to the page. Molecular images can definitely be detected at the left part of the image but are not clear at the right. It is observed here also that the molecular orientations are reversed across the line XX' in the figure. The molecular image encircled with a black line in the figure shows a prominent contrast. It can be considered that the molecule in the dislocation core is subject to intermolecular forces which differ from the forces expected to act in the perfect part of the crystal. As a result the molecule in the core is considered to assume an orientation different from the surroundings. The image in Fig. 6 supports this view. The molecular inversion and the indistinctness of the molecular images a little way from the dislocation core can be interpreted on the same principle as that used above to explain the molecular images at the grain boundary. At an edge dislocation, one molecular layer is removed from a part of the crystal. In the part lacking one molecular layer the residual molecules are displaced to fill up the empty part. The displacement along the slip plane XX' is about a half period near the dislocation and results in the same relationship among the slipped and unslipped molecules as that in the boundary between two grains slipping a half period along the boundary. Although the inversion of the molecular orientation near the edge dislocation is necessary for the close packing of phthalocyanine molecules, it becomes unfavourable at the crystal part where the deformation due to the dislocation is relaxed, *i.e.* in the crystal lattice away

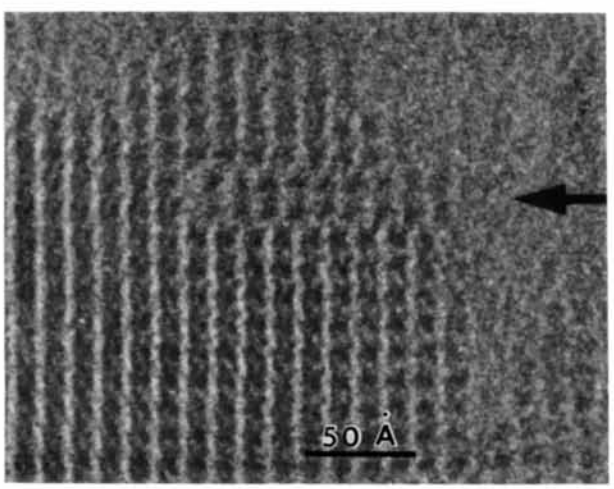

Fig. 5. An example of a bulk defect. At the arrowed part a small crystallite composed of eighteen molecular columns can be observed with a different molecular orientation from the surroundings.

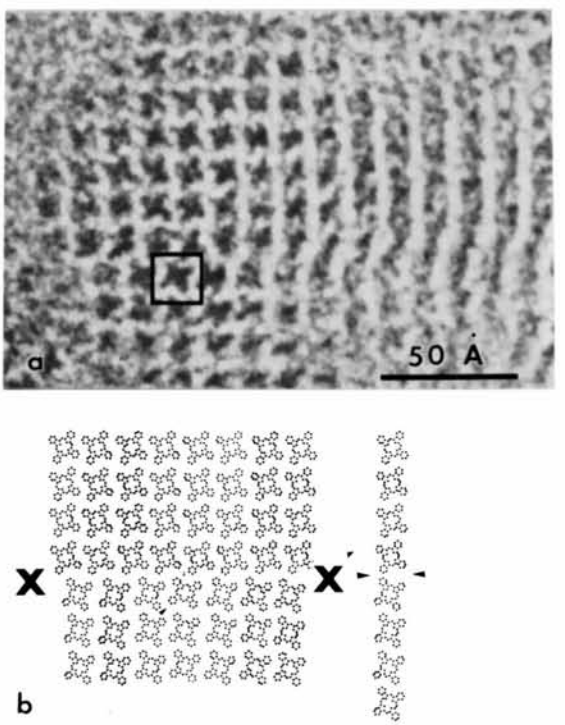

Fig. 6. Molecular arrangement around an edge dislocation (*a*) and its schematic representation (*b*).

from the dislocation. The recovery of a perfect lattice around the deformation is impossible owing to the steric hindrance at the interface on the slip plane resulting from the molecular inversion, as shown in Fig. 6(*b*). The unclearness of molecular images at the right part of the crystal displayed in Fig. 6 shows that at such a position, much disorder is introduced, resulting in the orientational rearrangement of molecules.

(3) *Twin structure*

The mechanism of twin formation in an organic crystal can be explained by anisotropy in intermolecular forces and anisotropy of molecular shape. A twinned crystal of the α-III form of Zn-Phc is shown in Fig. 7, which is the projection on the (010) plane. This crystal is composed of two kinds of molecular layers, which have different molecular orientations (Kobayashi, Fujiyoshi, Iwatsu & Uyeda, 1981). The molecular images are well defined in the first layers whereas in the second layers the images are not well resolved as a result of a superposition of molecules located at two different lattice sites. It can be seen in Fig. 7 that in the left and the right parts of the crystal the direction of the *a* axis is reversed with the *c* axis remaining the same. The twin plane is the (100) plane, and one extra molecular layer can be observed on the twin boundary. The situation of the boundary seems to be the same in nature as that in the grain boundary shown in Fig. 3. The origin of the twin structure can be considered as follows. Assuming the (100) plane as the growth front and taking the molecular symmetry into consideration, there are many possible positions for a new molecule coming to join the growth front. When the addition of the molecule occurs with the orientation *A*, as exhibited in Fig. 8, the crystal will normally grow, while when the molecule joins with the orientation *B* twinning occurs from this lattice point. Around a molecule at the corner of a crystal, there are more possible sites for the molecule to assume. In any case, the differences in free energy associated with the addition of a molecule in each of such sites are considered not to be so large in the growing crystal that not only can twin formation occur but also various polymorphs can be easily produced in the phthalocyanine crystals.

(4) *Growth mechanisms and quasi-amorphous state of phthalocyanine*

The growth of a thin crystalline film investigated here presents a new mechanism where the production of a one-dimensional crystal, a molecular column, in a growing crystal plays an important role in the growth process. Fig. 9 is an image of α-III form of a 50 Å thick Zn-Phc crystal seemingly in process of growing. The growth process can be suspended by stopping the supply of molecules to the growing crystal and introducing air into the sublimation vessel to suppress the movement of molecules on the substrate surface. The dark dots show different contrasts at the edge or

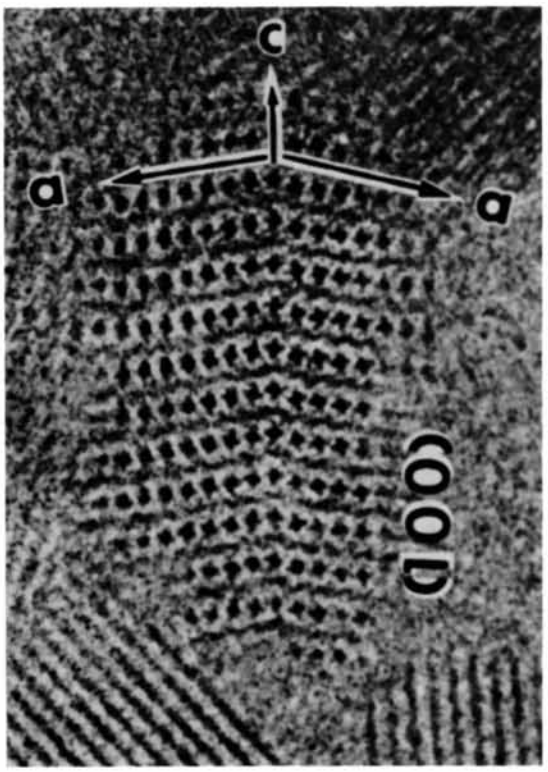

Fig. 7. A twinned crystal of the α-III form of Zn-Phc. The twin boundary is an (001) plane.

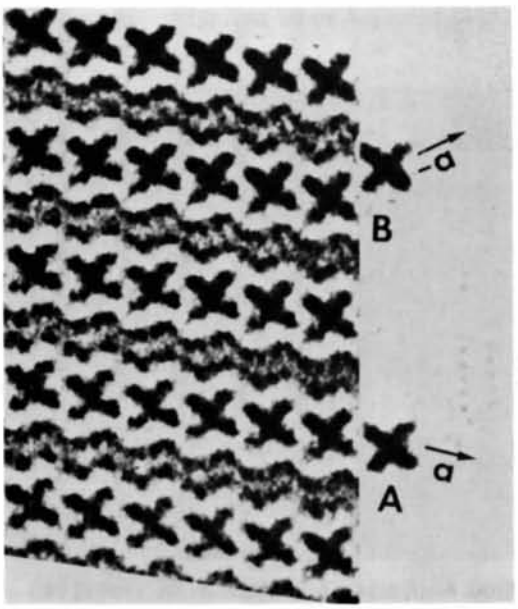

Fig. 8. Twin formation is initiated by the addition of a molecule at site *B*.

corner of the crystal or at sites away from the edges. Although the distribution of such molecular images is random at the arrowed part A, each image can be clearly observed with enough contrast to be detected. The contrast indicates that each molecular image does not correspond to the image of a single molecule but to the projection of a molecular column along its axis. That is, the linear crystals or molecular columns are formed before the three-dimensional crystal is constructed. The formation of the linear crystals can be observed in the early stage of the crystal growth. Figs. 10 and 11 show the images of very thin films of Pt-Phc whose mean thicknesses are 10 and 25 Å respectively. The thicknesses correspond to about one and two molecular layers when the molecules are deposited on the substrate with their molecular planes perpendicular to the substrate. In Fig. 10 no definite crystallite but molecular columns of different lengths can be observed as bellows-like images. The column axis lies parallel to the substrate. It may well be wondered whether the images of such molecular columns are those of single columns or those of projections of plural columns piled up along the electron beam direction. However, it is reasonable to consider that the images are given by single columns for the following reasons. The first reason is that the mean film thickness measured is less than that of monomolecular layer. The film is observed to be composed of uniformly distributed molecules or molecular columns and not composed of island

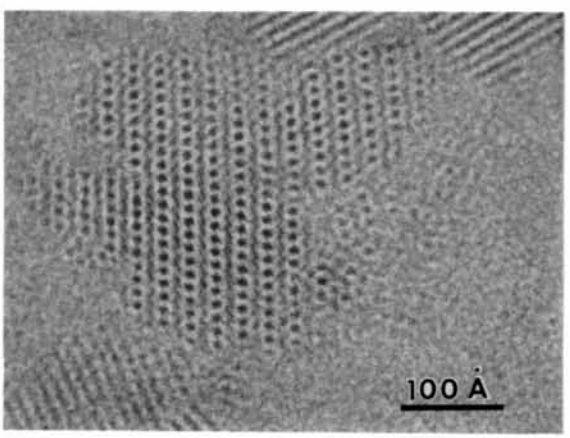

(*a*)

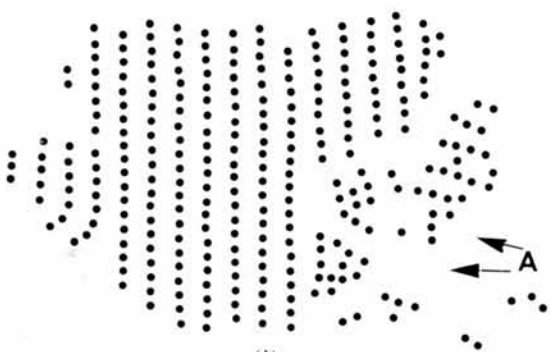

(*b*)

Fig. 9. (*a*) An image of a Zn-Phc crystal showing the growing process. Each black dot in (*b*) corresponds to a molecular image in the projection *A* in Fig. 2. The most faint contrast may represent a single molecule.

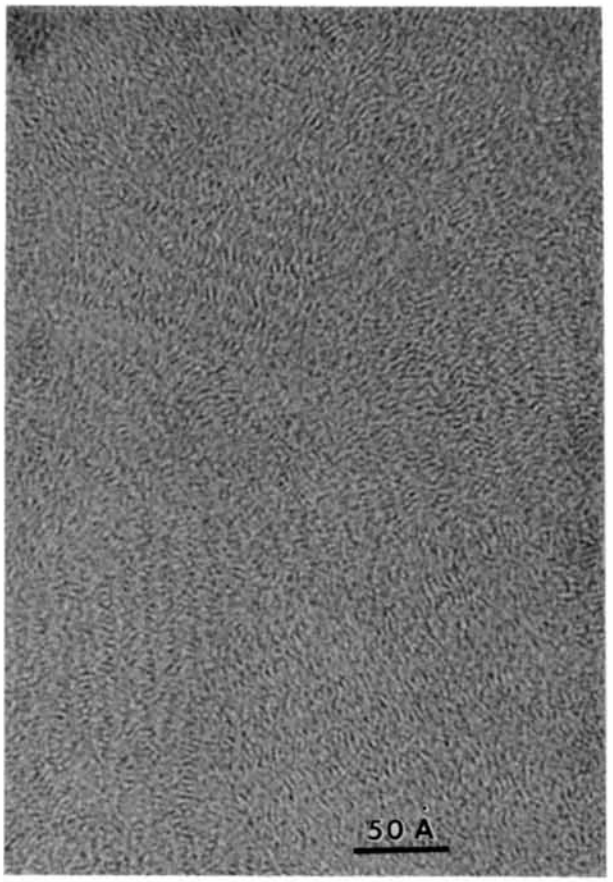

Fig. 10. Image of a quasi-amorphous state of Pt-Phc 10 A in thickness. Linear crystals can be observed.

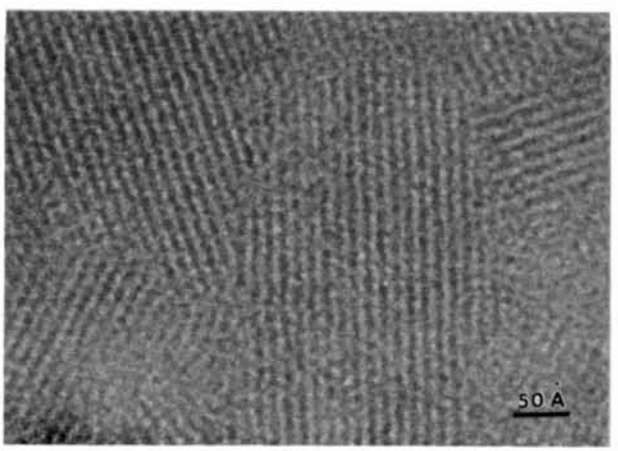

Fig. 11. At the thickness of 25 Å, crystal formation can be seen.

crystallites. The second reason is that it is unlikely that the disordered molecules in columns are piled up regularly to give definite molecular images. The image shown in Fig. 11 is obtained with a film of Pt-Phc whose thickness is two molecular layers. The molecular columns are ordered in this film. The well arranged crystal parts increase when the film thickness increases. In these cases, disorder is observed as a bend of the column, which results in the deterioration of image quality as can be seen in Fig. 9, where the molecular columns are projected along the column axis. The disordered states displayed in Fig. 9 and Fig. 10 can be considered to result from the lack of kinetic energy for surface diffusion of the molecule necessary for crystallization on the substrate, because the deposition was carried out at room temperature, at which the phthalocyanine molecule does not have sufficient energy for surface diffusion. The process of crystal growth of phthalocyanine may be considered as follows. The cohesive energy of phthalocyanine molecules due to π-electronic interaction is anisotropic and acts more strongly to build a molecular column. When the column grows to a certain extent, the attractive force between columns becomes strong and they condense side by side and make a crystal, as illustrated in Fig. 12. The contrast differences in each molecular image in Fig. 9 suggest that the length of the column is not constant. The images in Figs. 9 and 10 are obvious proofs for the concept that formation of linear crystal, molecular column, precedes the formation of three-dimensional crystals.

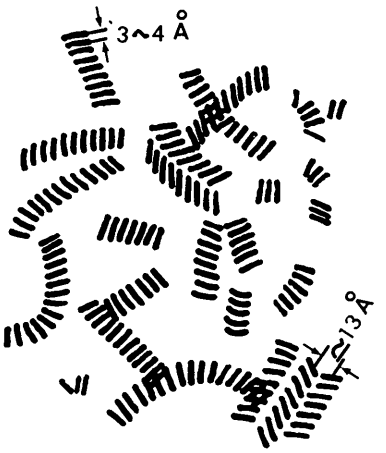

Fig. 12. Schematic representation of the initial state of the crystal formation.

References

BROWN, C. J. (1968). *J. Chem. Soc. A*, pp. 2488–2493, 2494–2498.

FRYER, J. R. (1977). *Inst. Phys. Conf. Ser.* No. 36, pp. 423–424.

FUJIYOSHI, Y., KOBAYASHI, T., ISHIZUKA, K., UYEDA, N., ISHIDA, Y. & HARADA, Y. (1980). *Ultramicroscopy*, **5**, 459–468.

KOBAYASHI, T., FUJIYOSHI, Y., IWATSU, F. & UYEDA, N. (1981). *Acta Cryst.* A**37**, 692–697.

WILLIAMS, J., THOMAS, J. M., WILLIAMS, J. O. & HOBBS, L. W. (1975). *J. Chem. Soc. Faraday Trans.* II, **71**, 138–145.

Acta Cryst. (1982). A**38**, 362–371

A Study of Generalized Intensity Statistics: Extension of the Theory and Practical Examples

BY URI SHMUELI

Department of Chemistry, Tel-Aviv University, 69978 Ramat Aviv, Israel

(*Received* 27 *August* 1981; *accepted* 22 *December* 1981)

Abstract

Generalized probability density functions, cumulative distribution functions and moments of the normalized structure amplitude $|E|$, depending on space-group symmetry of the crystal and on the composition of the asymmetric unit, were extended to include the tenth moment of $|E|$ and five-term expansions. The formalism was also simplified and is presented in a concise and unified form. The equations linking the formalism to practical problems, the composition and space-group terms, are discussed from a practical point of view and a convenient implementation of the above statistics in a computer program is indicated. The generalized cumulative distributions of $|E|$ and of the normalized intensity $z = |E|^2$ are compared with corresponding distributions based on five published structures, each containing one outstandingly heavy atom (Pt, Rh and

0567-7394/82/030362-10$01.00